Complex-Forming Poly(oxyethylene)/Poly(acrylic acid) Interpenetrating Polymer Networks. 2. Function as a Chemical Valve

Shiro Nishi[1] and Tadao Kotaka*

Department of Macromolecular Science, Faculty of Science, Osaka University, Toyonaka, Osaka 560, Japan. *Received June 26, 1985*

ABSTRACT: An interpolymer complex of poly(oxyethylene) (POE) and poly(acrylic acid) (PAA) was incorporated into an interpenetrating polymer network (IPN) to design a special function membrane. The membrane may be called a *chemical valve*, because its permeability can be controlled reversibly by adjusting the chemical environment such as pH and ionic strength of the buffer. This behavior is presumably due to opening and closing of channels respectively by protonation and deprotonation of the PAA network, followed by reversible formation and dissociation of the complex due to hydrogen bonding between POE and PAA networks within the IPN membrane. Thus, not only the flux but also the size of the solute macromolecules permeable through the membrane could be varied reversibly by changing the pH of the medium. A simple model was presented to simulate this chemical-valve function. The model semiquantitatively described the size and number of the channels in the IPN membrane opened and closed by pH control.

Introduction

This article is concerned with a special function membrane prepared from an interpenetrating polymer network (IPN) of poly(oxyethylene) (POE) and poly(acrylic acid) (PAA).[2-6] The polymer pair is capable of forming an *interpolymer-complex* POE/PAA through hydrogen bonds between the ether oxygen and carboxylic acid hydrogen.[7] Such a complex can be dissociated by changing, for example, the pH of the medium. However, such a polymer complex alone cannot be used as a membrane, because once the complex is dissociated it is difficult to be reformed reversibly in the medium. Therefore, we incorporated this POE/PAA complex into an *interpenetrating polymer network* (IPN)[8-10] to design a special function membrane.[2-6]

A lightly cross-linked POE/PAA IPN membrane[2] having equimolar composition was particularly intriguing because the complex formation and dissociation within the membrane could be controlled reversibly by adjusting its chemical environment such as the pH and ionic strength of the medium.[3-6] The IPN membrane swelled by more than 30 times when the pH was changed from a low to a high value and deswelled when the pH was brought back to the low value again.[3] The membrane also exhibited a mechanochemical response: When the membrane was equilibrated in a buffer of neutral pH with a small weight attached, it stretched and subsequently retracted reversibly upon addition of an alkali or acid to the buffer.[3,4]

Thus, we attempted to utilize this complex-forming IPN system as a permselective membrane, and we tested whether the flux and the permeability of solute molecules of different sizes can be altered by changing the pH of the solution.[6]

Experimental Section

Materials. Transport experiments were carried out on three different types of membranes: a cross-linked poly(oxyethylene) (cr-POE), a cross-linked poly(acrylic acid) (cr-PAA), and a POE/PAA IPN membrane of equimolar composition. The preparation and characterization of these membranes were reported previously.[2,5] Here, we describe the procedures only briefly.

To prepare a cr-POE membrane, we cross-linked hydroxyl-terminated POE prepolymer (POE 6000) with a trifunctional isocyanate, (2-isocyanato)ethyl-(2,6-diisocyanato)hexanoate (IDI), supplied by Toray Industries, Inc. We mixed 40 mol % of IDI with POE 6000 (so that the OH/NCO ratio is 1) in a sealed polymerization cell and kept it at 80 °C for 24 h and at room temperature for 10 more days to complete the reaction.[5] To prepare a cr-PAA membrane, we mixed acrylic acid monomer (AA) with 0.5 wt % initiator, α,α'-azobis(isobutylonitrile) (AIBN), and a 1 mol % cross-linker, ethylene diacrylate (EDA), and allowed the mixture to react at 80 °C for 48 h.[5]

To prepare a POE/PAA IPN membrane, we soaked cr-POE for a given period of time (usually a few minutes) in the AA/EDA/AIBN mixture so that the equimolar amount of AA was taken up by the membrane. The membrane swollen with the monomer mixture was kept in the polymerization cell at 80 °C for 48 h to obtain an IPN membrane with the equimolar AA-to-oxyethylene ratio.[5] The thickness of the membranes was typically 0.20 mm.

The obtained IPN membrane showed a single sharp glass transition at around 310 K, as revealed by the dynamic mechanical measurement and differential scanning calorimetry.[2,5] The infrared (IR) spectra showed existence of hydrogen bonds due to the carboxylic acid/ether complex.[5] These results suggest that the IPN membrane is a homogeneous system, stabilized by complex formation through hydrogen bonding between the ether oxygens of POE and the carboxylic acid hydrogens of PAA.[5]

Test liquids used for the transport experiments[6] were pure water, HCl, and NaOH aqueous solutions, sodium phosphate buffer of various pH and ionic strengths I, and 1 wt % solutions of homopoly(oxyethylenes) (POE) dissolved in the same phosphate buffer of pH 2.5 or 7.0 and I = 0.01. The water was distilled and then deionized before use.

We used the following 10 homo-POE samples for the transport experiments. Six low molecular weight samples were purchased from Nakarai Chemicals Co. Three of these low molecular weight samples were fractionated with benzene and n-hexane.[11,12] The other three samples were purified with hot toluene and n-hexane.[11,12] Three high molecular weight samples were Polyoxy samples (Union Carbide Corp.) obtained through the courtesy of Prof. Guy C. Berry, Carnegie–Mellon University. Another high molecular weight sample was obtained through the courtesy of Prof. Akira Takahashi, Mie University. These four high molecular weight samples were used as received.

For the four low molecular weight samples the average molecular weights M were determined by cryoscopy in benzene as 401, 666, 1190, and 2580. For the other six intermediate to high molecular weight samples the M were determined by intrinsic viscosity measurements at 20 or 25 °C in benzene.[13,14] Gel permeation chromatography (GPC Model HLC-801A, Toyo Soda Mfg. Co.) was also conducted by using a low-angle laser light scattering monitor (Model LS-8, Toyo Soda Mfg. Co.). The carrier solvent was tetrahydrofuran.[11,12] The values of M determined for these six samples were 6.5×10^3, 25.5×10^3, 187×10^3, 358×10^3, 1.50×10^6, and 2.38×10^6.

Methods. In order to determine the solution viscosity as well as the intrinsic viscosity $[\eta]$ of the homo-POE samples in the sodium phosphate buffer, we carried out viscosity measurements at 25 °C, usually starting from a 1 wt % solution and successively

0024-9297/86/2219-0978$01.50/0

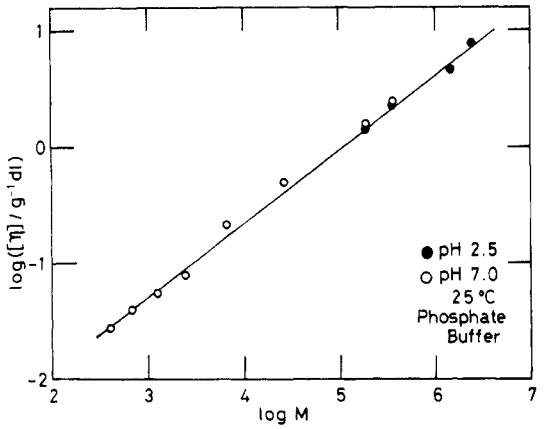

Figure 1. Plot of log $[\eta]$ vs. log M of homo-POE at 25 °C in the sodium phosphate buffer of $I = 0.01$ and at pH 2.5 (filled circles) and pH 7.0 (open circles).

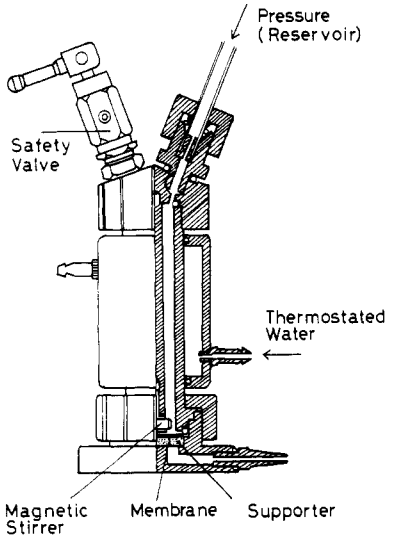

Figure 2. Ultrafiltration cell assembly employed for the transport experiments.

diluting it to infinite dilution. For the measurements, we employed conventional Ubbelohde type viscometers of various capillary size. The pH of the buffer was adjusted to 2.5 or 7.0, and the ionic strength $I = 0.01$ in accordance with the conditions for the transport experiments.

Figure 1 shows a double logarithmic plot of the $[\eta]$ data vs. molecular weight M of the POE samples in the sodium phosphate buffer. The best fit for the data gives a Mark–Houink–Sakurada equation

$$[\eta] = (7.94 \times 10^{-4})M^{0.62} \quad (1)$$

for both pH 7.0 and 2.5 data at 25 °C.

Swelling tests were carried out at 25 °C on cr-POE, cr-PAA, and the POE/PAA IPN specimens. In one series of tests, the free specimens were swollen in sodium phosphate buffers of various pH but with a constant ionic strength of $I = 0.01$. In another series, the specimens were swollen in the sodium phosphate buffer of pH 7.0 but with various I. The degree of swelling, $Q = W_s/W_p$, was defined by the ratio of the weights W_s to W_p of the specimen after and before the swelling experiment, respectively.

For the liquid-transport experiments, we employed an ultrafiltration cell system (UHP-25, Toyo Filter Paper Co., Ltd.) made from Teflon and equipped with a water jacket. A sketch of the cell is shown in Figure 2. The effective radius of the membrane mounted on the holder was 20.0 mm. Each membrane was conditioned in advance with sodium phosphate buffer of pH 7.0 and $I = 0.01$, sandwiched between two porous Teflon filters (PF-2, Toyo Filter Paper Co., Ltd.), mounted on the ultrafiltration cell,

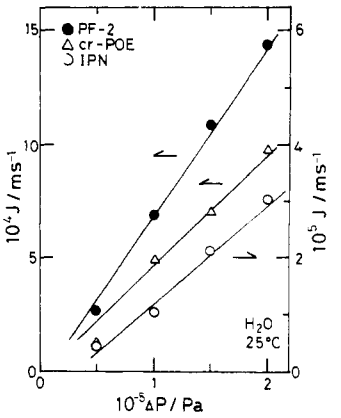

Figure 3. Plot of the flux J vs. the applied pressure ΔP for pure water at 25 °C through the prous Teflon filter PF-2 (closed circles), cr-POE (triangles), and the POE/PAA IPN membrane (open circles).

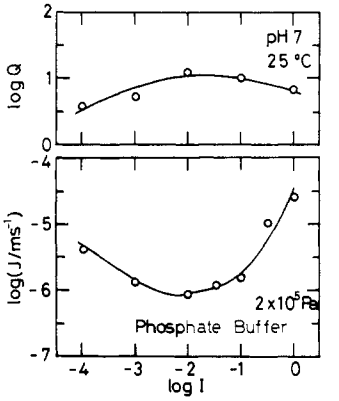

Figure 4. Plots of log Q and log J (under $\Delta P = 200$ kPa) vs. log I at 25 °C of sodium phosphate buffer of pH 7.0 for the IPN membrane.

and subjected to the liquid-transport test at 25 °C under argon pressure ΔP of 50–200 kPa.[6]

The pH measurements were made at 25.0 °C with an ion analyzer (SelectIon 5000, Beckman Instruments) and a combination electrode (Futura Combination Electrode No. 39504, Beckman Instruments).

Results

Figure 3 shows the pressure ΔP dependence of the flux J (m s^{-1}, volume/unit area and time) of distilled and deionized water through the porous filter PF-2 alone and with a cr-POE or an IPN membrane. The flux J for the PF-2 filter alone (without any test membrane inserted) is much larger than that for the cr-POE or IPN membranes. Thus, the PF-2 support hardly affected the permeability of the membranes. According to the nonequilibrium thermodynamics,[15] the transport of a solution is given as

$$J = L_f(\Delta P - \sigma\Delta\pi) \quad (2)$$

where L_f and σ are the filtration and reflection coefficients, respectively and $\Delta\pi$ is the osmotic pressure difference across the membrane. Ehen both solute and solvent are permeable through the membrane, σ is equal to 0. In contrast, when only the solvent is permeable, σ is 1. The values of L_f (in m^2 kg^{-1} s) for pure water were determined to be 75×10^{-10} for PF-2, 49×10^{-10} for cr-POE, and 1.8×10^{-10} for the IPN membrane from the slopes of the plots shown in Figure 3. The value of L_f for cr-POE is about 27 times larger than that for IPN.

Figure 4 shows the dependence of Q and J of the IPN membrane on the ionic strength I for the sodium phosphate buffer at pH 7.0. With increasing I, Q increased and

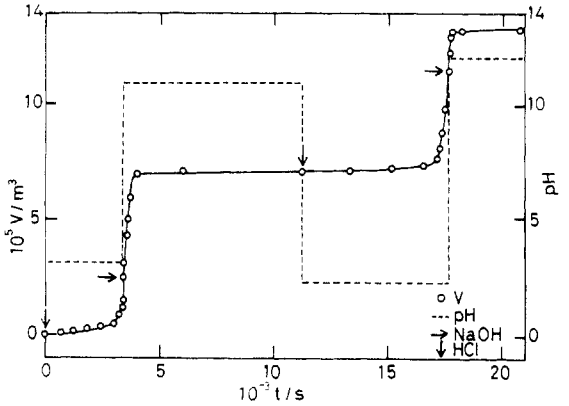

Figure 5. Change with time t of efflux volume (open circles) and pH (dashed line) of water at 25 °C by adding HCl (↓) and NaOH (→) alternately.

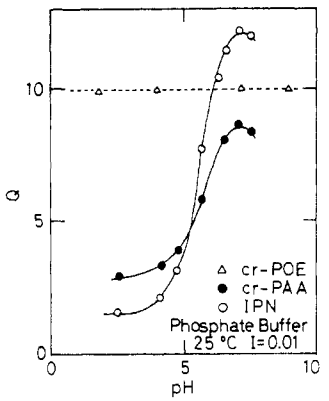

Figure 6. Plots of the swelling ratio Q vs. pH of free cr-POE (triangles), cr-PAA (closed circles), and the IPN membrane (open circles) for sodium phosphate buffer of I = 0.01 at 25 °C.

passed a maximum at I = 0.01, where the J decreased and passed a minimum. Thus, I = 0.01 was chosen as the standard condition for the subsequent experiments involving the sodium phosphate buffer.

Figure 5 shows the change with time t of the total volume, V, and pH of water transported through the IPN membrane upon addition of HCl or NaOH alternately. The test was carried out at 25 °C under 200 kPa argon atmosphere. For the IPN membrane of the effective radius of 20.0 mm and (dry) thickness 0.20 mm, water permeated at first very slowly at a flow rate of approximately 0.17×10^{-3} cm^3 s^{-1}. However, about 50 min after we added HCl to reduce the pH to about 3, the flow rate of water increased almost 1000 times to the order of 0.19 cm^{-3} s^{-1}. We then added NaOH to increase the pH to about 11 and observed that the flow rate reduced to the original low value again within a few minutes. These processes could be repeated reversibly by adding HCl and NaOH alternately to the feed solution.

A more quantitative observation was made on swelling and transport experiments of the sodium phosphate buffer at various pH. We compared the swelling ratios Q of free specimens of IPN, cr-POE, and cr-PAA in the sodium phosphate buffer of various pH and I = 0.01. The results are summarized in Figure 6 in the plot of Q vs. pH of the buffer at 25 °C.

Transport experiments of the sodium phosphate buffer at various pH and I = 0.01 were conducted on the IPN, cr-POE, and cr-PAA membranes. Figure 7 shows the plot of log J vs. pH of the buffer at 25 °C under the pressure difference P = 200 kPa.

For cr-POE, both Q and J were relatively large and independent of the pH of the buffer. In contrast, for

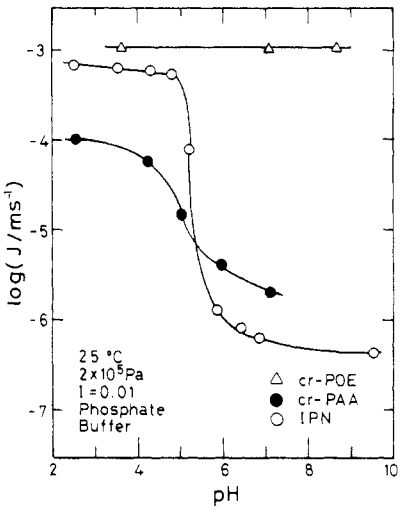

Figure 7. Plots of log J vs. pH of cr-POE (triangles), cr-PAA (closed circles), and the IPN membrane (open circles) fixed in the ultrafiltration cell for sodium phosphate buffer of I = 0.01 at 25 °C.

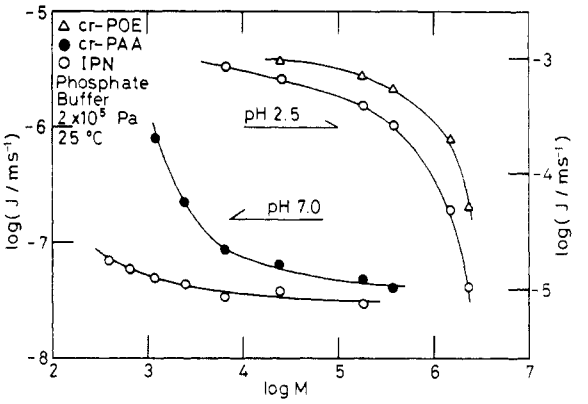

Figure 8. Plots of log J vs. log M of the solute homo-POE samples dissolved in sodium phosphate buffer of I = 0.01 through cr-POE at pH 2.5 (triangles), the IPN membrane at pH 2.5 and 7.0 (open circles), and cr-PAA at pH 7.0 (closed circles) at 25 °C under ΔP = 200 kPa.

cr-PAA and the IPN membrane both Q and J strongly depended on pH and I. These changes upon pH change took place reversibly within a relatively narrow range of pH. The Q for the free cr-PAA specimen was low at low pH but increased 3-fold at high pH, while the flux J for the fixed cr-PAA membrane was high at low pH but decreased roughly by a factor of 50 at high pH.

The Q of the free IPN specimen at low pH was smaller than that of cr-PAA but increased by a factor of 10 at pH 7.0. The flux J for the fixed IPN membrane was very large at low pH but decreased by a factor of almost 1500 as the pH increased. As seen in Figures 6 and 7, the changes in Q and J of the IPN membrane upon pH change were far larger than those of cr-PAA.

A more striking effect of pH change was seen in the flux J of 1 wt % POE solutions of different M dissolved in the buffer of pH 2.5 or 7.0. Figure 8 shows double logarithmic plots of the flux J vs. M for cr-POE at pH 2.5, the IPN membrane at pH 2.5 and 7.0, and cr-PAA at pH 7.0.

The flux J of the 1 wt % POE solutions through the cr-POE membrane was unchanged by pH and was very high at either pH 2.5 or 7.0. The flux J for the solution containing the lowest M solute was as high as that of the buffer alone but decreased with increasing M of the solute.

The flux J of the POE solutions through the IPN membrane at pH 2.5 was also high, and the dependence

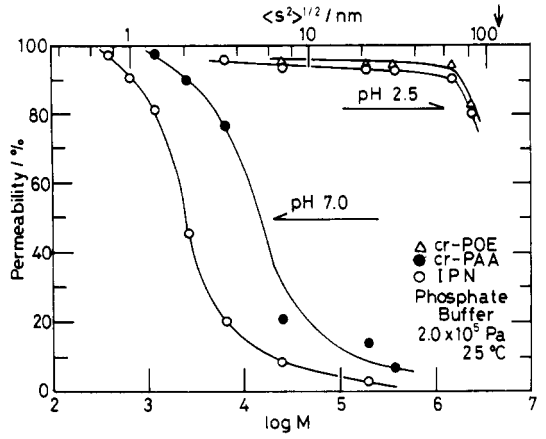

Figure 9. Plots of the permeability percent vs. log M of the solute homo-POE samples dissolved in sodium phosphate buffer of I = 0.01 through cr-POE at pH 2.5 (triangles), the IPN membrane at pH 2.5 and 7.0 (open circles), and cr-PAA at pH 7.0 (closed circles) at 25 °C under ΔP = 200 kPa. The arrow at the upper right corner indicates the average pore radius r of the IPN membrane at pH 2.5. (See text.)

on the solute M was similar to that of the cr-POE membrane. However, at pH 7.0 the flux J became very small. It was smaller by a factor of 10 than that of the buffer even for the solution containing the lowest M solute.

These tendencies were more or less the same for the cr-PAA membrane. The flux J at pH 7.0 was much smaller than that for cr-POE but somewhat larger than that for the IPN membrane. The flux J decreased rapidly with increasing M of the solute. However, it was difficult to carry out the measurement, because at low pH the cr-PAA membrane fixed on the cell was weak and often broken before the steady-state transport was reached, especially for the viscous POE solutions. However, the flux J appeared to be as high as that for the IPN membrane at low pH.

Another striking effect of pH change was seen in the permeability of the solute POE molecules through these membranes. Figure 9 compares the permeability percent of the solute POE through cr-POE at pH 2.5, the IPN membrane at pH 2.5 and 7.0, and cr-PAA at pH 7.0. The 100% permeability implies that all the solute molecules passed through the membrane.

For the cr-POE membrane at any pH, and also for the IPN membrane at pH 2.5, the solute permeability was more than 90% for all the POE samples except for the one with the highest M. On the contrary, the IPN membrane at pH 7.0 rejected more than 50% of the solute with M above 2600. The cr-PAA membrane at pH 7.0 also showed more than 50% rejection for the solute with M above 6000. However, at pH 2.5 we observed a peculiar behavior. When a POE solution was transported through the cr-PAA membrane at pH 2.5, most of the solutes were at first trapped by the membrane and did not pass through. At a later stage, the membrane behaved as a semi-IPN membrane in which only PAA chains were cross-linked. However, it was not possible to compare quantitatively the cr-PAA and IPN membranes because the former was very weak at this low pH.

A similar observation was reported by Osada[16] on a poly(methacrylic acid) (cr-PMAA) membrane cross-linked with glycerol. When the membrane was treated with 2.5% POE solution of $M = 2 \times 10^4$ before the permeation experiment, the membrane exhibited a high flux and allowed nearly 100% permeation of amylase (M = 45 000) and other low M globular proteins, but 80% rejection of albumin (M = 67 000). In contrast, the untreated membrane showed a very low flux for any protein solutions as well as the buffer.

Discussion

Mechanism of Liquid Transport through the IPN Membrane. It is known that the transport mechanism of a liquid through a nonporous membrane in which the liquid can dissolve is governed by dissolution and diffusion processes. The rate of the liquid transport is given by the average diffusion coefficient multiplied by the solubility of the liquid toward the membrane. In such cases, the flux J often takes a maximum under the condition where the solubility of the liquid to the membrane takes a maximum. However, this was not the case for the cr-PAA and IPN membranes, as seen in Figure 4 which shows the J and Q vs. I plots for the IPN membrane at pH 7.0.

In Figures 6–9, we notice more striking differences between the transport behavior of the cr-PAA and IPN membranes at different pH and also between that of the cr-POE membrane. The Q and J of the cr-POE membrane were high and independent of pH. The permeability of the solute POE molecules was also high except for the one with the highest M. On the contrary, the Q and J as well as the solute permeability of the cr-PAA and IPN membranes were strongly dependent on pH. For these membranes, the J and the solute permeability were low when the Q was high, but high when the Q was low.

It should be again noted that each membrane was first equilibrated and swollen at pH 7.0 in an unrestrained condition and subsequently fixed on the ultrafiltration cell. Thus, at the beginning the cr-PAA and IPN membranes were in the swollen state at high pH, where the PAA network was deprotonated. Moreover, in the swollen IPN membrane, the POE/PAA complex dissociated and the two networks interpenetrated each other. This interpenetrating network conformation may retard the liquid flow more strongly than either the cr-POE membrane or the swollen cr-PAA membrane alone, as seen in Figure 7.

For the swollen cr-PAA and IPN membranes at pH 7.0, the flux J and the solute permeability for the POE solutions decreased rapidly with increasing M of the solute. This is presumably because at pH 7.0 the membranes rejected the solute substantially (10%–20% of the solute of M = 1190 and as much as 85%–98% of the solute of $M = 1870 \times 10^3$), and the resultant concentration polarization retarded the transport of the solution through these membranes.

It is known that mixing aqueous solutions of POE and PAA at low pH leads to formation of an equimolar POE/PAA complex containing hydrogen bonding.[7,16,17] If the conditions were properly chosen, such a complex is reversibly dissociated and re-formed by adjusting the pH of the medium.[7,16,17] Reversible complex formation and dissociation by chaning the pH of the buffer were observed also in the POE/PAA IPN membrane. This observation was confirmed also on a POE/PAA semi-IPN membrane, in which only PAA chains were cross-linked.[4] The uncross-linked POE chains complexed with the PAA network at low pH were not extractable, but those not complexed with the PAA network at pH 7.0 were gradually lost from the semi-IPN membrane.[3-6]

When pH was lowered to 2.5, the cr-PAA membrane became protonated and deswelled. However, the fixed membrane could not shrink. Thus, channels or pores of a relatively large size should be created to release internal stresses in the membrane. As the result, the flux J was increased substantially.

In addition to this phenomenon, the protonated PAA network in the IPN membrane formed a complex with the

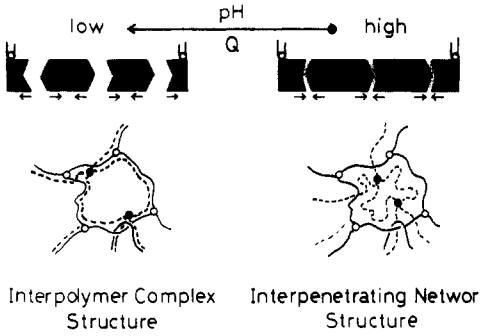

Figure 10. Schematic models showing the structures and the chemical-valve function of the POE/PAA IPN membrane when the pH of the medium is changed.

POE network.[3] Thus, the IPN membrane deswelled more than the cr-PAA membrane alone. The complex formation may create pores of a larger size (and possibly a larger number of pores, too) in the IPN membrane than those existing in the cr-PAA membrane.

Changes in the pH result in protonation and deprotonation of the PAA network, which in the case of the IPN membrane induce complex formation and dissociation. The resultant conformational changes, in turn, tend to open and close a valve (or valves), allowing the solution to flow through the channels or to stop. The situation is schematically shown in Figure 10. Thus, we may call these membranes a *chemical valve*.[16]

The cr-PAA membrane alone should also exhibit a chemical-valve function not only for the buffer but also for the permeation of water-soluble polymers which do not form complexes with PAA. Such a function should be due mainly to the polyelectrolytic nature of the membrane. However, the cr-PAA membrane may exhibit a perculiar behavior at pH 2.5 when POE or other complex-forming polymer solutions are permeated. Under such a condition, the solute POE molecules often form complexes with the cr-PAA membrane. Thus, the membrane behaves as a semi-IPN in which only PAA chains are cross-linked. Its behavior is probably similar to that of the full-IPN membrane, except that the uncross-linked component is lost at high pH. However, these could not be confirmed for the present cr-PAA membrane because of its fragility at low pH.

The channel flow mechanism explains why not only the flux but also the size of the solute molecules permeable through these membranes can be changed by the pH change and also why the changes are more pronounced in the case of the IPN membrane rather than the cr-PAA membrane alone.

This mechanism also explains the slow response of the membrane toward an acid but the rapid response toward an alkali. In other words, it was slow to open but quick to close the channels. For the chemical-valve function to operate, there are several relevant processes involved to open the channels: (1) diffusion of H^+ into the membrane; (2) protonation of COO^- groups of the PAA chains; (3) deswelling of the membrane, accompanying conformational rearrangement of the network chains; and (4) formation of interpolymer complex. In contrast, the processes involved to close the channels are (5) diffusion of OH^- into the membrane; (6) dissociation of the POE/PAA complex; and (7) deprotonation of COOH groups of the PAA network accompanying (8) conformational change due to the Coulombic interaction among the COO^- groups to fill the pores of the membrane. Steps 4 and 6 are, of course, absent in the cr-PAA membrane.

Bendnar and Morawetz[17] reported the kinetics of cooperative complex formation and dissociation of POE and PAA in a 1 M NaCl aqueous solution at 25 °C. They estimated the rate constant k_1 of the complex formation at pH 2.7 to be 0.11–0.57 s^{-1} and the rate constant k_{-1} of the complex dissociation at pH 6.37 to be 51.8 s^{-1}. These reactions cannot be the rate-determining steps, because the observed rates for the IPN membrane were much slower than these rate constants.

In view of the rapid rates of the neutralization and dissociation of low molecular weight carboxylic acids, the protonation and deprotonation of the COOH groups are also unlikely to be the rate-determining steps. Instead, the rate-determining steps might be attributed to the rates of the transport of H^+ and OH^- ions to reach the relevant sites in the membrane or the rates to replace the buffer in the membrane at high pH by the one at low pH and vice versa. The OH^- ions migrate by a rapid flow of the buffer through the open channels, while the H^+ ions must migrate by diffusion through the matrix or the closed channels of the swollen membrane. This explains, at least, the faster rate of the valve-closing process over the valve-opening process. However, for the IPN membrane at low pH, the flux J was 1500 times larger than that at high pH, while the observed rate of the valve-closing process was faster only by a factor of 10 than the rate of the valve-opening process. Therefore, these processes are also unlikely to be the rate-determining steps.

The remaining possibility, then, may be the rates of conformational rearrangement of the network chains in the membrane at low pH to that at high pH and vice versa. The membrane must be in a relaxed condition at high pH, but have large internal stresses in the deswollen state at low pH. The stress-buildup process should then proceed more slowly than the stress-releasing process, as observed in our preliminary experiments on the mechanochemical reaction of the similar IPN membranes.[3]

Modeling of the Chemical-Valve Function. To explain the chemical-valve function mentioned above, we introduce the following simple model. At high pH, channels are not open, so that the transport of the solution proceeds essentially by permeation through the swollen matrix of the membrane. For simplicity, we call this a diffusion flow J_D. (This diffusion flow may take place through much smaller pores.) In contrast, at low pH, channels are now open as a result of deswelling of the fixed, preswollen membrane. We assume that n channels of the average radius r are created in the unit area of the membrane. We further assume that the volume fraction of these created channels corresponds to the difference between the swelling ratios $Q_{7.0}$ and $Q_{2.5}$ at pH 7.0 and 2.5, respectively. We then have

$$\frac{(\text{unit area} - n\pi r^2)d_{2.5}}{(\text{unit area})d_{7.0}} = \frac{Q_{2.5}}{Q_{7.0}} \tag{3}$$

where $d_{2.5}$ and $d_{7.0}$ are the effective thickness of the deswollen and swollen membrane at the respective pH. If we assume uniform swelling and deswelling of the fixed membrane, the effective thickness d at a given pH may be given as

$$Q = (d/d_0)^3 \tag{4}$$

with d_0 being the thickness of the dry membrane. (Alternatively, we may assume the fixed membrane would not change its thickness; thus, $d_{2.5} = d_{7.0}$.

In contrast, the flux $J_{2.5}$ at pH 2.5 is the sum of the flux J_p through the created channels and the diffusion flow J_D through the membrane matrix. Assuming that the latter

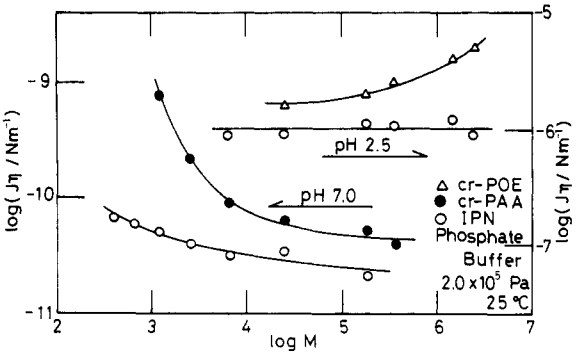

Figure 11. Plots of log ($J\eta$) vs. log M for 1 wt % POE solutions through the same membranes shown in Figure 8. Note the transport behavior through the IPN membrane at pH 2.5 obeys the channel flow model of eq 5.

is equal to the flux $J_{7.0}$ at pH 7.0 and that the two transport paths are aligned parallel, we

$$J_{2.5} = J_p + (Q_{2.5}/Q_{7.0})J_{7.0} \quad (5)$$

Finally, we introduce a most crude assumption of the Hagen–Poiseuille law for the channel flow; when a liquid of the viscosity η flows through n channels of the effective radius r and path length l under the pressure difference of ΔP, the flux J_p may be given as

$$J_p = n\pi r^4 \Delta P/(8\eta l) \quad (6)$$

(More precisely, r^4/l must be a complicated average $\langle r^4/l \rangle$ over all the channels existing in the membrane.) The pore radius r may be regarded as the permeability limit for the solute permeating through the membrane. In principle, these equations may apply to any membranes if the contribution of the reflection term in eq 1 is negligible and the liquid does not interact with the membrane.

Correlating the effective length l of the channels to the membrane thickness d, we may estimate the model parameters n and r from the Q and J data using eq 3–6. The path length l may be of the same order of or somewhat longer than d. (However, it cannot be very much longer than d.) Thus, as the simplest case, we assume l to be equal to d at the given pH and obtained $n = 2.3 \times 10^{13}$ m^{-2} and $r = 120$ nm for the buffer.

The same calculation may be applied to the permeation of the POE solutions, since the IPN membrane at pH 2.5 rejects less than 10% solute, except the solute of the highest M, and the effect of concentration polarization should be small. For the POE solutions having the viscosity differing by a factor of 100, we obtained the parameter $r = 125$–135 nm with $n = 2.3 \times 10^{13}$.

The relation between $[\eta]$ and the root-mean-square radius of gyration $\langle s^2 \rangle^{1/2}$ of the solute macromolecules may be calculated by the Flory–Fox viscosity equation[18]

$$[\eta] = (3.1 \times 10^{22})\langle s^2 \rangle^{3/2}/M \quad (7)$$

From $[\eta]$ data given by eq 1 and 7, we calculated $\langle s^2 \rangle^{1/2}$ of the permeating solute, as shown on the abscissa of Figure 9. The arrow at the upper right corner of Figure 9 indicates the value of $\langle s^2 \rangle^{1/2}$ corresponding to r for the buffer. It appears that the value of r is at least of the right order of magnitude for the IPN membrane at low pH.

Because the model is extremely crude and simple, the above coincidence of the parameters might be just fortuitous. However, an essential point of the model is that the $J_p\eta$ under a constant ΔP defined by eq 6 reflects only the characteristics of the membrane but not of the permeating liquid. In Figure 11, we tested the J data according to eq 6.

The flux $J_{2.5}$ through the IPN membrane at pH 2.5 may be approximately equal to J_p given by eq 6, but the flux $J_{7.0}$ through the cr-PAA and IPN membranes at pH 7.0 is not, because the effect of solute rejection and concentration might not be negligible for these systems. As anticipated, the plot was independent of the solute M only for the IPN membrane at pH 2.5, and those at pH 7.0 depended on M.

It should be noted that the cr-PAA membrane also exhibited a chemical-valve function, although to a lesser extent due to its polyelectrolytic nature. However, it appears that the complex formation and dissociation between the PAA and POE chains enhanced significantly the changes in the solvent flux as well as the permeability of macromolecular solutes through the IPN membrane and also imparted strength to the membrane, as judged from the present data shown in Figures 6–9. This conclusion is supported also by our preliminary observation on the cr-PAA membrane with POE solutions at low and high pH and Osada's results[16] on the cr-PMAA membrane complexed with POE for permeation of some globular protein solutions.

The cr-POE membrane also exhibited a large flux and a high permeability, independent of the pH of the buffer. This behavior suggests that the cr-POE membrane also possesses pores or channels of considerably large size, to which the channel flow model can be applied. We estimated the size and number of such pores, using eq 3–6, as $n = 1.0 \times 10^{13}$ and $r = 170$ nm for the buffer and $r = 170$ nm for the POE solution of $M = 25.5 \times 10^3$ to $r = 240$ nm for $M = 2.38 \times 10^6$. Since the cr-POE membrane is soft, the pore size and distribution may be affected by external mechanical stresses. This might be the reason that the log $J\eta$ value increases with M of the solute, because a more viscous solution containing a higher M solute may exert larger shear stresses at the channel wall of the cr-POE membrane. However, it should be pointed out that these channels, even if they exist, do not constitute a chemical valve, because neither the size nor the number of these channels of the cr-POE membrane can be controlled by changing the pH and I of the buffer.

Acknowledgment. This work was supported by the Ministry of Education, Science, and Culture (Mombusho) through Grant 543026 given to T.K. during 1980–1982. Financial support was also given to T.K. from Yamada Science Foundation during 1984. We wish to express our sincere thanks for these supports.

Registry No. (POE)·(IDI) (copolymer), 97042-87-0; (AA)·(EDA) (copolymer), 52641-03-9.

References and Notes

(1) Present address: NTT Musashino Electrical Communication Laboratories, Nippon Telegraph and Telephone Corp., Musashino-shi, Tokyo 180, Japan.
(2) Nishi, S.; Adachi, H.; Kotaka, T. *Rep. Progr. Polym. Phys. Jpn.* **1981**, *24*, 5, 299. *Ibid.* **1983**, *26*, 317. Adachi, H.; Nishi, S.; Kotaka, T. *Polym. J. (Tokyo)* **1982**, *14*, 985.
(3) Nishi, S.; Adachi, H.; Kotaka, T. *Rep. Progr. Polym. Phys. Jpn.* **1982**, *25*, 97. *Ibid.* **1983**, *26*, 215.
(4) Nishi, S.; Kotaka, T. *Rep. Progr. Polym. Phys., Jpn.* **1982**, *25*, 419.
(5) Nishi, S.; Kotaka, T. *Macromolecules* **1985**, *19*, 1519. *Rep. Progr. Polym. Phys. Jpn.* **1984**, *27*, 3, 315.
(6) Nishi, S.; Kotaka, T. *Rep. Progr. Polym. Phys. Jpn.* **1984**, *27*, 267.
(7) Smith, K. L.; Winslow, A. E.; Peterson, D. E. *Ind. Eng. Chem.* **1959**, *51*, 1361.
(8) Sperling, L. H. *Macromol. Rev.* **1977**, *12*, 141.
(9) Klempner, D.; Frisch, K. C. "Polymer Alloys"; Plenum Press: New York, 1977.

(10) Sperling, L. H. "Interpenetrating Polymer Networks and Related Materials"; Plenum Press: New York, 1981.
(11) Suzuki, T.; Kotaka, T. *Macromolecules* **1980**, *13*, 1495. *Polym. J. (Tokyo)* **1983**, *15*, 15.
(12) Se, K.; Adachi, K.; Kotaka, T. *Polym. J. (Tokyo)* **1981**, *13*, 1009.
(13) Sadron, C.; Rempp, P. *J. Polym. Sci.* **1658**, *24*, 127.
(14) Allen, G.; Booth, C.; Hurst, J.; Jones, M. N.; Price, C. *Polymer* **1967**, *8*, 391.
(15) See, for example, Katchalsky, A.; Curren, P. F. "Nonequilibrium Thermodynamics in Biophysics"; Harvard University Press: Cambridge, MA, 1965.
(16) Osada, Y.; Takeuchi, Y. *J. Polym. Sci., Polym. Lett. Ed.* **1981**, *19*, 303. *Polym. J. (Tokyo)* **1983**, *15*, 279.
(17) Bendnar, B.; Morawetz, H.; Shafer, J. A. *Macromolecules* **1984**, *18*, 72.
(18) See, for example, Flory, P. J. "Principles of Polymer Chemistry"; Cornell University Press: Ithaca, NY, 1953.

Studies on Functional Latices. Catalytic Effects of Histamine-Containing Polymer Latex–Copper(II) Complex on the Oxidation of Ascorbic Acid

Zonghua Sun,*† Changhong Yan,† and Hiromi Kitano‡

Chengdu Institute of Organic Chemistry, Academia Sinica, China, and Department of Polymer Chemistry, Kyoto University, Japan. *Received June 10, 1985*

ABSTRACT: The catalytic activity of the histamine-containing polymer latex–Cu(II) complex (abbreviated latex-His–Cu(II)) on the oxidation of ascorbic acid is examined. The latex catalyst shows a so-called Michaelis–Menten type saturation behavior. The Michaelis constants (K_m) and reaction rate constants of the latex catalyst–substrate complex (k_2) are obtained by double reciprocal plots at various temperatures. K_m of the latex-His–Cu(II) system is much larger (about 90 times) than that of the poly(L-histidine)–Cu(II) system because of the electrostatic repulsion between the anionic substrate and the carrier latex. k_2 of the latex system, however, is about 10 times larger than that of poly(L-histidine)–Cu(II), which suggests the cooperative action of the Cu(II)–imidazole complex with neighboring carboxyl groups on the latex surface. Reusability and storage stability of the latex catalyst are also examined.

Most enzymes that act as catalysts in organisms are spherical proteins consisting of repeatedly folded polypeptide chains. In recent years, interest has been shown in studying polymer latex microspheres as enzyme-like hydrolytic catalysts,[1] electrically charged polymer catalysts,[2] and carriers of immobilized enzymes[3,4] and immunoglobulin.[5] It is well-known that cupric ion exists at the active site of some oxidases, such as tyrosinase.[6] To mimic enzymatic oxidation systems, the catalytic behavior of polymer–copper(II) complex in the oxidation reaction has been extensively studied.[7] Pecht et al.[8] found that the oxidation of ascorbic acid was effectively catalyzed by the poly(L-histidine)–Cu(II) complex (PLH–Cu(II)). This complex was homogeneous in water solution and exhibited a Michaelis–Menten type behavior. There is no report on the polymer latex–metal complex as an oxidase-like catalyst. In this paper, we report the enzyme-like catalytic effects of the histamine-containing polymer latex–Cu(II) complex in the oxidation of ascorbic acid.

Experimental Section

Materials. Styrene (St) and acrylic acid (AA) were purified by vacuum distillation. Divinylbenzene (DVB) was washed with 2 N NaOH aqueous solution to remove the inhibitor. Potassium peroxydisulfate (KPS), ascorbic acid, acetic acid, sodium acetate (NaAc), and cupric sulfate were analytical-grade reagents and were used without further purification. Histamine (His) and 1-ethyl-3-(3-(dimethylamino)propyl)carbodiimide hydrochloride (EDC) were obtained from Sigma Chemical Co. (St. Louis, MO) and used without further purification. Doubly distilled water was used in all reactions.

Copolymerization of Latices. Polymer latices were prepared by emulsifier-free copolymerization as follows: 149 mL of water was poured into a three-necked 250-mL round-bottomed flask equipped with a mechanical stirrer, a reflux condenser, and a N_2-inlet tube. The flask was thoroughly filled with pure nitrogen gas kept at 70 °C. A total 28.3 mL of St, 0.62 mL of AA, and 0.25 mL of DVB were poured into the flask, and 105 mg of KPS was finally added as initiator. The mixture was stirred at 240–250 rpm for 5 h while N_2 was continuously passed through the flask. After the copolymerization was complete, the temperature of the solution was raised to 80 °C, and the reflux condenser and N_2-inlet tube were taken away to evaporate unreacted monomers. Two hours later heating and stirring of the solution were stopped. The polymer latex solution was cooled to room temperature, passed through a 120-mesh Nylon filter cloth, and poured into a glass bottle. The latex particles were purified by ion-exchange resin and dialyzed for 1 week against distilled water.

The composition of the polymer latex particles determined from elemental analyses was C, 91.56; H, 7.74; O, 0.70. The amount of carboxyl group in the latex particles was estimated to be 0.22 mmol/g latex. The average diameter of the particle was estimated to be 2500 Å from electron micrographs with a JEM-100CX electron microscope. The dispersion parameter ($\hat{\delta}/\bar{x}$) was calculated to be 0.014 with

$$\hat{\delta} = [\sum_{i=1}^{n}(x_i - \bar{x})^2/(n-1)]^{1/2} \quad (1)$$

where $\hat{\delta}$ is mean square deviation, x_i is the diameter of the particles, and $\bar{x}$ is the average diameter of the particles. Figure 1 clearly shows that the latex particles have excellent monodispersity and a "clean" surface.

Preparation of Latex-Conjugated Ligands and Their Complex with Cu(II). Histamine was coupled to the latex surface by the EDC method[9]: 50 mL of latex suspension (12.2% solids) was mixed with 150 mL of H_2O, and the pH of the mixture was adjusted to 4.2 with 0.1 N HCl aqueous solution. Then 0.79 g of histamine and 1.30 g of EDC were added, and the pH of the solution was kept at 4.2 for 1 h at room temperature. The reaction mixture was stored at 4 °C under continuous stirring. After 56 h, the reaction mixture was centrifuged for 15 min at 15 000 rpm. The latex particles coupled with histamine were then washed with distilled water three times by centrifugation and were finally suspended in 200 mL of H_2O.

† Academia Sinica.
‡ Kyoto University.

0024-9297/86/2219-0984$01.50/0